



# $^{11}\text{Be}(\beta p)$ , a quasi-free neutron decay?



K. Riisager<sup>a,\*</sup>, O. Forstner<sup>b,c</sup>, M.J.G. Borge<sup>d,e</sup>, J.A. Briz<sup>e</sup>, M. Carmona-Gallardo<sup>e</sup>, L.M. Fraile<sup>f</sup>, H.O.U. Fynbo<sup>a</sup>, T. Giles<sup>g</sup>, A. Gottberg<sup>e,g</sup>, A. Heinz<sup>h</sup>, J.G. Johansen<sup>a,1</sup>, B. Jonson<sup>h</sup>, J. Kurcewicz<sup>d</sup>, M.V. Lund<sup>a</sup>, T. Nilsson<sup>h</sup>, G. Nyman<sup>h</sup>, E. Rapisarda<sup>d</sup>, P. Steier<sup>b</sup>, O. Tengblad<sup>e</sup>, R. Thies<sup>h</sup>, S.R. Winkler<sup>b</sup>

<sup>a</sup> Department of Physics and Astronomy, Aarhus University, DK-8000, Aarhus C, Denmark

<sup>b</sup> Faculty of Physics, University of Vienna, Währinger Strasse 17, A-1090 Wien, Austria

<sup>c</sup> Stefan-Meyer-Institut für subatomare Physik, Austrian Academy of Sciences, A-1090 Wien, Austria

<sup>d</sup> ISOLDE, PH Department, CERN, CH-1211 Geneve 23, Switzerland

<sup>e</sup> Instituto de Estructura de la Materia, CSIC, E-28006 Madrid, Spain

<sup>f</sup> Grupo de Física Nuclear, Universidad Complutense de Madrid, CEI Moncloa, E-28040 Madrid, Spain

<sup>g</sup> EN Department, CERN, CH-1211 Geneve 23, Switzerland

<sup>h</sup> Fundamental Fysik, Chalmers Tekniska Högskola, SE-41296 Göteborg, Sweden

## ARTICLE INFO

### Article history:

Received 7 February 2014

Received in revised form 21 February 2014

Accepted 31 March 2014

Available online 4 April 2014

Editor: V. Metag

### Keywords:

Beta decay

Halo nucleus

$^{11}\text{Be}$

## ABSTRACT

We have observed  $\beta^-$ -delayed proton emission from the neutron-rich nucleus  $^{11}\text{Be}$  by analyzing a sample collected at the ISOLDE facility at CERN with accelerator mass spectrometry (AMS). With a branching ratio of  $(8.3 \pm 0.9) \cdot 10^{-6}$  the strength of this decay mode, as measured by the  $B_{GT}$ -value, is unexpectedly high. The result is discussed within a simple single-particle model and could be interpreted as a quasi-free decay of the  $^{11}\text{Be}$  halo neutron into a single-proton state.

© 2014 The Authors. Published by Elsevier B.V. This is an open access article under the CC BY license (<http://creativecommons.org/licenses/by/3.0/>). Funded by SCOAP<sup>3</sup>.

## 1. Introduction

Beta-minus decay and proton emission take a nucleus in almost opposite directions on a nuclear chart, so  $\beta^-$ -delayed proton emission (where beta decay feeds excited states that subsequently emit a proton) is forbidden in all but a few nuclei where it is heavily suppressed as the available energy is [1]  $Q_{\beta p} = 782 \text{ keV} - S_n$ , where  $S_n$  is the neutron separation energy of the nucleus. We describe here an experiment to detect this decay mode from the one-neutron halo nucleus  $^{11}\text{Be}$  that is believed to be the most favourable case [2,3] due to the single-particle behaviour of halo nuclei [4–6] that may favour this decay mode and due also to the relatively long half-life that is caused by the normal beta-decay of  $^{11}\text{Be}$  being hindered since a level inversion gives it a  $1/2^+$  ground state rather than a  $1/2^-$ .

Beta-delayed particle emission is in general a prominent decay mode for nuclei close to the dripline, see [7,8] for recent reviews. The energetically open channels for  $^{11}\text{Be}$  are  $\beta\alpha$ ,  $\beta t$ ,  $\beta p$  and  $\beta n$  with corresponding  $Q$ -values of [9]  $2845.2 \pm 0.2 \text{ keV}$ ,  $285.7 \pm 0.2 \text{ keV}$ ,  $280.7 \pm 0.3 \text{ keV}$  and  $55.1 \pm 0.5 \text{ keV}$ . The low decay energy implies that the branching ratio for beta-delayed proton emission is low, typical estimates are slightly above  $10^{-8}$  [3]. To detect the process experimentally, it is therefore essential to keep contaminants at a very low level.

The  $\beta p$  decay mode may be expected preferentially in one-neutron halo nuclei, partly due to the requirement of low neutron separation energy, partly due to the more pronounced single-particle behaviour of halo nuclei. Two-neutron halo nuclei are in a similar way candidates for beta-delayed deuteron emission, which has so far been observed only in the nuclei  $^6\text{He}$  and  $^{11}\text{Li}$  [7,10]. For  $^{11}\text{Li}$  the decay has a branching ratio of order  $10^{-4}$ , the low value again caused by a small energy window, whereas cancellation effects reduces the branching ratio for  $^6\text{He}$  down to the  $10^{-6}$  level. It may be more useful to consider the standard measure for the strength of a decay, the reduced matrix element squared  $B_{GT}$ , that is found from the relation [7]

\* Corresponding author.

E-mail address: [kvr@phys.au.dk](mailto:kvr@phys.au.dk) (K. Riisager).

<sup>1</sup> Present address: Institut für Kernphysik, Technische Universität Darmstadt, D-64289 Darmstadt, Germany.

$$ft = \frac{K}{g_V^2 B_F + g_A^2 B_{GT}}, \quad (1)$$

where  $f$  is the beta-decay phase space,  $K/g_V^2 = 6144.2 \pm 1.6$  s and  $g_A/g_V = -1.2694 \pm 0.0028$ . Converting the observed spectra for beta-delayed deuteron emission from the two-neutron halo nuclei  ${}^6\text{He}$  [11] and  ${}^{11}\text{Li}$  [12] gives total  $B_{GT}$  values within the observed energy range of about 0.0016 and 0.75. (Note, however, that the  ${}^6\text{He}$  decay to the  ${}^6\text{Li}$  ground state has been described as an effective di-neutron to deuteron decay, it is a highly allowed transition with a  $B_{GT}$  of 4.7. This may be a reflection of a general trend for highly allowed decays to occur in very neutron-rich nuclei [13].) For comparison, the sum of  $B_{GT}$  for all currently known transitions in the  ${}^{11}\text{Be}$  decay is 0.27.

## 2. The experiment

### 2.1. General remarks

The radioactive  ${}^{11}\text{Be}$  nuclei were produced at the ISOLDE facility at CERN. Searching for protons with a kinetic energy of a few hundred keV with relative intensity  $10^{-8}$  is challenging in a radioactive beam environment, so we instead detect the decay product,  ${}^{10}\text{Be}$  with a half-life of  $1.5 \cdot 10^6$  y, that exists only in minute quantities on earth. To reach the needed sensitivity we must employ state-of-the-art AMS. It is also crucial to limit the amount of contaminants in the samples, so sample collection took place at ISOLDE's high-resolution mass separator. The resolution from the magnetic separation stage is supplemented by the electrostatic beam transport at ISOLDE similar to, but at lower resolution than, the separation stages in AMS facilities. A first attempt was made in 2001 and the results were published recently [3]. The signal was not sufficiently strong to be clearly separated from background and gave a  $\beta\beta$  branching ratio of  $(2.5 \pm 2.5) \cdot 10^{-6}$ . This is compatible with zero, but the uncertainty implies that an upper limit is significantly above the published theoretical expectations. Due to improvements both in production of  ${}^{11}\text{Be}$  and AMS detection of  ${}^{10}\text{Be}$ , the current collection was performed in December 2012 and resulted in three samples.

### 2.2. Sample collection

The  ${}^{11}\text{Be}$  activity was produced by bombarding a UC target with 1.4 GeV protons. The products were ionized in a laser ion source, which provided element selectivity, mass separated in the ISOLDE high-resolution separator, and guided through several collimators to the collection point where they were implanted at 60 keV in a small copper plate ( $15 \times 20 \times 2$  mm). A high-purity coaxial Ge-detector placed 40 cm downstream behind a lead shielding monitored the collection rate. The Ge-detector was energy and efficiency calibrated with standard sources of  ${}^{60}\text{Co}$ ,  ${}^{152}\text{Eu}$  and  ${}^{228}\text{Th}$ . The main lines in the  $\gamma$  spectrum recorded during  ${}^{11}\text{Be}$  collection are the 2124 keV line from the decay of  ${}^{11}\text{Be}$  and the 511 keV line from positron annihilation. The overall efficiency at 2124 keV is found to be  $(2.0 \pm 0.2) \cdot 10^{-5}$ . A second line from the decay at 2895 keV was also used to check the overall amount of  ${}^{11}\text{Be}$ . The two determinations gave about the same precision, the one from the 2124 keV line being dominated by systematic uncertainties in the efficiency and the one from the 2895 keV being dominated by statistical uncertainties, and were internally consistent leading to a final value for the amount of collected  ${}^{11}\text{Be}$  in the main sample (S1) of  $(1.47 \pm 0.14) \cdot 10^{12}$ . This includes a correction for dead time of 2.8%, determined from the ratio of accepted to total number of triggers.

As cross-checks two other samples were collected: sample S2 at the mass position of  ${}^{11}\text{Li}$  (0.02 mass units heavier than  ${}^{11}\text{Be}$ )

where an upper limit of  $3 \cdot 10^6$  could be determined for the number of atoms collected (corresponding to a  ${}^{11}\text{Li}$  yield below 625/s which is reasonable) and, for one second only, sample S3 at the  ${}^{10}\text{Be}$  mass position where an estimate of the current of 3.5 pA (uncertain by a factor two) converts into  $2.2 \cdot 10^7$  atoms. From previous yield measurements  ${}^{10}\text{Be}$  is known to be the dominant component of the mass 10 beam. According to SRIM calculations [14] about 6% of all Be ions implanted in Cu at 60 keV energy will backscatter out of the sample. Most of the backscattered ions are expected to remain close to the sample so  $\gamma$ -rays from their decays will be seen as well, although the decay products are not retained in the sample. This gives a correction which we estimate to be  $4 \pm 4\%$ .

### 2.3. Accelerator mass spectrometry

The  ${}^{10}\text{Be}$  accelerator mass spectrometry (AMS) measurements were performed at the Vienna Environmental Research Accelerator (VERA) at the University of Vienna. VERA is a dedicated AMS facility based on a NEC 3 MV pelletron tandem accelerator. A new scheme for  ${}^{10}\text{Be}$  using a passive foil absorber in front of a gas ionization chamber detector was employed. In this way the detection efficiency for  ${}^{10}\text{Be}$  atoms is increased significantly.

According to TRIM simulations [14] the maximum implantation depth of  ${}^{11}\text{Be}$  in our copper plate catcher was below 1  $\mu\text{m}$ . To reduce the amount of material to be dissolved only the surface layer of each irradiated copper plate was leached in nitric acid. A second leaching was performed to verify the blank level of the irradiated copper plate. The second leaching of sample S3 did not produce enough BeO for a measurement. For samples S1 and S2 the values of the second leachings were consistent with a blank sample. This shows that the material was sitting in the surface, as expected for an implanted sample, and not due to a bulk contamination. An amount of 359  $\mu\text{g}$  (uncertainty of 3%)  ${}^9\text{Be}$  carrier was added to the solution to reach a  ${}^{10}\text{Be}/{}^9\text{Be}$  isotopic ratio in the range of  $10^{-16}$ – $10^{-11}$ . After this step the  ${}^{10}\text{Be}/{}^9\text{Be}$  isotopic ratio is fixed for each sample. Even though the efficiency of the following chemical procedures is smaller than 100% this will affect both isotopes in the same way and the isotopic ratio remains unchanged. In the next step the solution was treated with ammonium hydroxide to precipitate the beryllium as beryllium hydroxide ( $\text{Be}(\text{OH})_2$ ). The dissolved copper remains in the solution in this step. The beryllium hydroxide was dried out by heating in an oven at 900  $^\circ\text{C}$  for at least 8 hours forming beryllium oxide ( $\text{BeO}$ ). The BeO powder was mixed 1 : 1 with high purity copper powder and pressed into sample holders and mounted together with standard and blank material in an MC-SNICS type cesium sputter ion source. The standard material has a known  ${}^{10}\text{Be}/{}^9\text{Be}$  isotopic ratio and is used to calibrate the AMS measurement. Blank is the pure phenakite material directly pressed into a sample holder. A separate sample, S-blank, went through the chemistry preparation to check for the amount of  ${}^{10}\text{Be}$  introduced during the chemical sample preparation.  $\text{BeO}^-$  was extracted from the ion source and stripped in the terminal of the tandem accelerator to  $\text{Be}^{2+}$ , resulting in a total ion energy of 2.4 MeV. After further mass separation by a sector magnetic analyzer and an electrostatic analyzer the remaining particles are sent to a gas ionization chamber detector with a two-split anode for particle identification. A silicon nitride foil stack as a passive absorber was installed in front of the detector. This foil stack prevents the isobaric background  ${}^{10}\text{B}$  from entering into the detector: The energy loss of boron in the foil stack is slightly larger compared to beryllium. By selecting the right foil thickness and carefully tuning the particle energy the boron ions are stopped in the foil stack whereas the beryllium ions can enter the detector.

**Table 1**

Results of the AMS measurement. S1 to S3 denote the irradiated samples. 1st and 2nd correspond to the first or second leaching. Blank and S-blank are control samples without activity.

Sample	$^{10}\text{Be}/^9\text{Be}$ ratio	$^{10}\text{Be}$ atoms
S1-1st	$(4.87 \pm 0.13) \cdot 10^{-13}$	$(1.17 \pm 0.05) \cdot 10^7$
S1-2nd	$(1.26 \pm 0.56) \cdot 10^{-15}$	$(3.03 \pm 1.35) \cdot 10^4$
S2-1st	$(3.10 \pm 0.94) \cdot 10^{-15}$	$(7.45 \pm 2.27) \cdot 10^4$
S2-2nd	$(4.4 \pm 3.1) \cdot 10^{-16}$	$(1.06 \pm 0.75) \cdot 10^4$
S3-1st	$(1.54 \pm 0.03) \cdot 10^{-12}$	$(3.70 \pm 0.13) \cdot 10^7$
S-blank	$(4.9 \pm 3.4) \cdot 10^{-16}$	$(1.18 \pm 0.82) \cdot 10^4$
Blank	$(1.3 \pm 1.3) \cdot 10^{-16}$	$(3.12 \pm 3.12) \cdot 10^3$

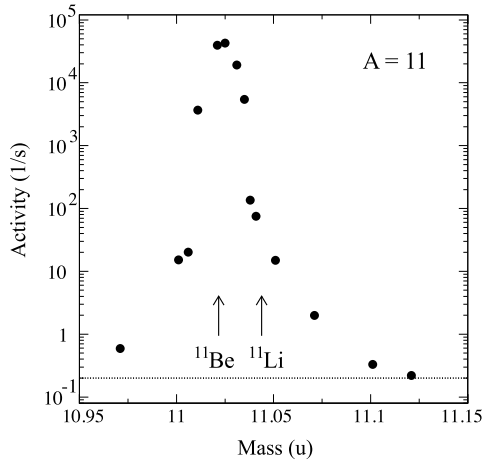


**Fig. 1.** Mass scan of the ISOLDE high-resolution separator across the  $^{11}\text{Be}$  position. The beta activity measured is shown versus the mass with the positions indicated for  $^{11}\text{Be}$  and the possible contaminant  $^{11}\text{Li}$ . The horizontal line marks the detection limit of 0.2/s.

A more thorough description of the AMS technique can be found e.g. in the review article [15].

The final results are given in Table 1. The amount of atoms in sample S3 agrees with the estimation from the implantation current. The  $^{10}\text{Be}$  seen in sample S2 is likely to come from the decay of  $^{11}\text{Li}$ , but the number is consistent with the lack of observed  $\gamma$ -rays from the decay. The number for sample S1, the  $^{11}\text{Be}$  sample, is  $(1.170 \pm 0.047) \cdot 10^7$ .

#### 2.4. Possible contaminants

Contaminations in our sample might arise due to tails of the neighbouring activities  $^{10}\text{Be}$  or  $^{11}\text{Li}$ , whose decay also produces  $^{10}\text{Be}$ . Both possibilities are ruled out by the low recorded number of atoms for the  $^{11}\text{Li}$  sample (S2). The ISOLDE mass separator profile was found by measuring the beta activity as the mass settings were changed around the nominal  $^{11}\text{Be}$  mass, see Fig. 1. The release function of this specific target and ion source combination was measured first, which allows to combine measurements with different collection times relative to proton impact on target. In this way the sensitivity was increased and the activity could be followed down to the  $10^{-5}$  level that occurred at a mass difference of 0.05 mass units. The only remaining way for  $^{10}\text{Be}$  to appear on the  $^{11}\text{Be}$  position is as the molecule  $^{10}\text{Be}^1\text{H}$ , but this molecule is unlikely to be formed in the target and to survive through the laser ion source since its ionization energy of 8.22 eV [16] is much higher than its dissociation energy of 3.26 eV. Nevertheless, we have re-checked the data from an earlier experiment on  $^{12}\text{Be}$  [17] and were able to put limits on the amount of  $^{11}\text{Be}^1\text{H}$  (from the  $\beta\alpha$  branch) that would correspond in our current case to a  $^{10}\text{Be}^1\text{H}$

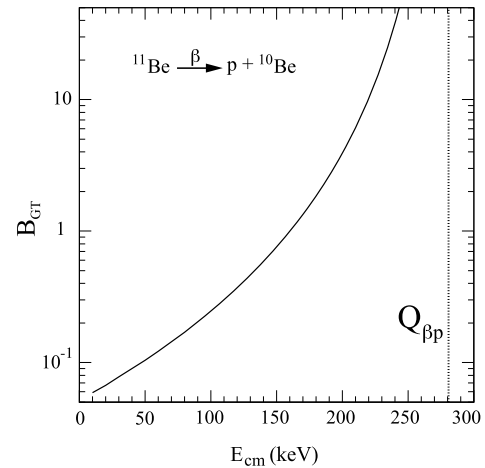


**Fig. 2.** The  $B_{GT}$  value to a narrow proton decaying resonance in  $^{11}\text{B}$  that will reproduce the measured  $\beta p$  branching ratio is shown as a function of the resonance energy. This estimate assumes that all other decay channels from the resonance are negligible.

intensity less than  $2 \cdot 10^{-6}$  of  $^{11}\text{Be}$ . Our conditions should be better, partly due to higher laser ionization power, partly due to the beam passing through a gas-filled RFQ cooler, both effects that would enhance molecular break-up. We therefore conclude that we have observed the  $^{11}\text{Be}(\beta p)$  decay via detection of the final nucleus  $^{10}\text{Be}$ . The observed intensity converts to a branching ratio of  $(8.3 \pm 0.9) \cdot 10^{-6}$ .

### 3. Discussion

The experimentally found branching ratio is surprisingly large, but consistent with the outcome of the first experiment. No existing calculation reproduces the magnitude. The calculations belong to two different types of models: sequential decay through a resonance or direct decay to the continuum. We first show in Fig. 2 the magnitude of  $B_{GT}$ , calculated from Eq. (1), that would be needed to explain the branching ratio if the decay proceeded through a narrow level to the  $p + ^{10}\text{Be}$  continuum. (As discussed below no existing level will have the required properties.) If on the other hand the decay went directly to the continuum and the strength in  $^{11}\text{Be}(\beta p)$  was as broadly distributed as in  $^{11}\text{Li}(\beta d)$  we would expect the  $B_{GT}$  within the  $Q$ -window to be less than 0.1, which would not be sufficient to explain the decay rate. We next explore the possibilities within a simple direct decay model for the decay along the lines of the calculations in [2,18], details of our calculations are reported elsewhere [19].

The basic assumption is that the beta decay proceeds as an essentially detached decay of the halo neutron into a proton. The initial and final state wavefunctions are calculated as single-particle states in square-well or Woods–Saxon potentials with the final state spectrum discretized by imposing a large confining radius at 1000 fm. The overlap of the wavefunctions gives the beta strength  $B_{GT}$  and the decay rate is found from Eq. (1). The final total branching ratio for beta-delayed proton emission depends strongly on the strength of the potential between the final state proton and  $^{10}\text{Be}$ . For most potential strengths the branching ratio will indeed be a few times  $10^{-8}$ , as in other calculations, but in a limited range the beta strength will be concentrated within the  $Q$ -window. Effectively, in this range the proton formed in the decay interacts strongly with the remaining  $^{10}\text{Be}$  and forms a resonance-like structure; as a consequence it emerges with a quite well defined energy. The branching ratios obtained for this set of parameters are shown in Fig. 3 as a function of the energy of the resonance.

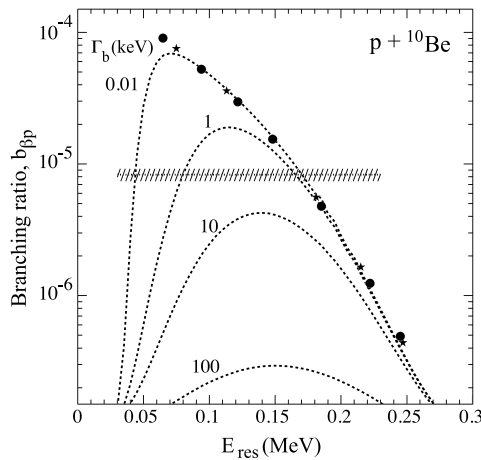


**Fig. 3.** The calculated branching ratio for decay into  $p + {}^{10}\text{Be}$  is shown as a function of the centre-of-mass energy of the resonance. The stars mark results of calculations with square well potentials, the filled circles are results from Woods–Saxon potentials. The curves arise from integrating the R-matrix expression in Eq. (2) for different widths for other decay channels. The horizontal band indicates the experimentally found branching ratio.

The simple model neglects isospin. The lowest  $T = 3/2$  states are situated slightly more than 1 MeV above the  $Q_{\beta p}$ -window. They are members of isospin multiplets that include the  ${}^{11}\text{Be}$  ground state and first excited state neutron halos. The data indicate [20] that the intermediate states ( $|T_z|$  of  $1/2$ ) in these multiplets have good total isospin rather than a composition with just one proton (or neutron) plus core. We therefore expect that realistic final state wave functions in our case, with  $T = 1/2$ , also should have good isospin. Standard isospin coupling then predicts that the state should be proton plus  ${}^{10}\text{Be}$  with weight  $2/3$  and neutron plus  ${}^{10}\text{B}(T = 1)$  with weight  $1/3$ . Our calculated decay probabilities must therefore be corrected by a factor  $2/3$ . A further reduction factor about 0.7 is due to the initial  ${}^{11}\text{Be}$  wavefunction containing several configurations [21]. The overall scaling factor on the theory, included in Fig. 3, is therefore about 0.5.

Since the direct decay model leads to a sequential picture with decays through a resonance we should now check whether this could be an established resonance in  ${}^{11}\text{B}$ . The known states [22] in this region mainly couple to the  $\alpha$ -particle channel (with partial widths around 100 keV) and only one, a state at  $11450 \pm 17$  keV, may have spin-parity that allows emission of an s-wave proton – the others will have angular momentum barriers that will suppress proton emission. Decays through levels that have other sizeable decay channels ( $\alpha$  emission or, for very narrow levels,  $\gamma$  emission; in principle triton emission could also occur) would therefore only contribute to the proton channel with probability  $\Gamma_p/\Gamma_{tot}$ . Since  $\Gamma_\gamma$  for the  $1/2^+$ ,  $T = 3/2$  state at 12.55 MeV (that apart from isospin should be similar in structure to our state) is about 10 eV [22], and even a small admixture into our state of other  $1/2^+$  levels is likely to give a  $\Gamma_\alpha$  at least of the same magnitude, we shall assume the width for other decay channels  $\Gamma_b = \Gamma_\gamma + \Gamma_\alpha$  to be larger than 0.01 keV.

To take these effects into account calculations were also made within the R-matrix approach [23], but in a simplified version where e.g. other decay channels are approximated as having a constant width  $\Gamma_\alpha$  over the energy window, see [19] for details. Converting the decay rate into a differential branching ratio gives the following expression:

$$\frac{db}{dE} = t_{1/2} \frac{g_A^2}{K} \frac{B_{GT} \Gamma_p / 2\pi}{(E_{res} - E)^2 + \Gamma_{tot}^2 / 4} f(Q - E), \quad (2)$$

where  $\Gamma_{tot} = \Gamma_b + \Gamma_p$ ,  $\Gamma_p = 2P\gamma^2$ ,  $P$  is the standard (energy-dependent) penetrability factor and  $\gamma^2$  the maximal reduced width. Integration over the  $Q$ -window gives the total branching ratios shown in Fig. 3 as a function of resonance position  $E_{res}$  for different values of  $\Gamma_b$ . The branching ratios agree well with the ones from the simple model. It is clear that all known levels are too wide to fit and that a  $\Gamma_b$  above 0.01 keV gives a lower limit on the  $B_{GT}$  of about 0.3 with an upper limit given by the theoretical maximum of 3.

#### 4. Conclusion

We have observed beta-delayed proton emission for the first time in a neutron-rich nucleus. The unexpectedly high decay rate can only be understood within current theory if the decay proceeds through a new single-particle resonance in  ${}^{11}\text{B}$  (i.e. coupling strongly to the proton channel and only weakly to other decay channels) that is strongly fed in beta-decay. The  $B_{GT}$ -value could be as high as 3 which is that of a free neutron decay. A natural interpretation would be peripheral beta decay of the halo neutron in  ${}^{11}\text{Be}$  into a single-proton state. This appears to be a simpler process than the  $\beta d$  decays of the two-neutron halo nuclei  ${}^6\text{He}$  and  ${}^{11}\text{Li}$ . Although the halo structure must be important for the  $\beta p$  decay mode, the large value of  $B_{GT}$  may be related to large values found in other (non-halo) near-dripline nuclei [13] and point to a more widespread change of beta-decay patterns at least in light nuclei in line with some predictions [24].

#### Acknowledgements

We thank the ISOLDE group for the successful operation of the HRS separator at very high resolution and Aksel Jensen for discussions on the theoretical interpretation. We acknowledge support from the European Union Seventh Framework through ENSAR (contract No. 262010), from Austrian Science Fund (FWF) P22164-N20, from Spanish MINECO through projects FPA2010-17142 and FPA2012-32443, and CPAN Consolider CSD-2007-00042.

#### References

- [1] B. Jonson, K. Riisager, Nucl. Phys. A 693 (2001) 77.
- [2] D. Baye, E.M. Tursonov, Phys. Lett. B 696 (2011) 464.
- [3] M.J.G. Borge, et al., J. Phys. G 40 (2013) 035109.
- [4] A.S. Jensen, K. Riisager, D.V. Fedorov, E. Garrido, Rev. Mod. Phys. 76 (2004) 215.
- [5] I. Tanihata, H. Savajols, R. Kanungo, Prog. Part. Nucl. Phys. 68 (2013) 215.
- [6] K. Riisager, Phys. Scr. T 152 (2013) 014001.
- [7] M. Pfützner, M. Karny, L.V. Grigorenko, K. Riisager, Rev. Mod. Phys. 84 (2012) 567.
- [8] B. Blank, M.J.G. Borge, Prog. Part. Nucl. Phys. 60 (2008) 403.
- [9] M. Wang, et al., Chin. Phys. C 36 (2012) 1603.
- [10] T. Nilsson, G. Nyman, K. Riisager, Hyperfine Interact. 129 (2000) 67.
- [11] D. Anthony, et al., Phys. Rev. C 65 (2002) 034310.
- [12] R. Raabe, et al., Phys. Rev. Lett. 101 (2008) 212501.
- [13] M.J.G. Borge, et al., Z. Phys. A 340 (1991) 255.
- [14] J.F. Ziegler, Particle interactions with matter, <http://www.srim.org>, 20 January 2014.
- [15] L.K. Fifield, Rep. Prog. Phys. 62 (1999) 1223.
- [16] S. Bubin, L. Adamowicz, J. Chem. Phys. 126 (2007) 214305.
- [17] C.Aa. Diget, et al., Nucl. Phys. A 760 (2005) 3.
- [18] M.V. Zhukov, B.V. Daniilin, L.V. Grigorenko, J.S. Vaagen, Phys. Rev. C 52 (1995) 2461.
- [19] K. Riisager, Nucl. Phys. A 925 (2014) 112–125.
- [20] B. Jonson, K. Riisager, Philos. Trans. R. Soc. Lond. A 356 (1998) 2063.
- [21] K.T. Schmitt, et al., Phys. Rev. Lett. 108 (2012) 192701.
- [22] J.H. Kelley, et al., Nucl. Phys. A 880 (2012) 88.
- [23] F.C. Barker, E.K. Warburton, Nucl. Phys. A 487 (1988) 269.
- [24] H. Sagawa, I. Hamamoto, M. Ishihara, Phys. Lett. B 303 (1993) 215.